A study on reflection of moving intrinsic localized modes at a junction of two different nonlinear lattices

Masayuki Kimura,† Ryou Tsujisaka,‡ Takashi Hikihara,† Yoshiharu Taniguchi,‡ and Yasuo Matsushita¶

†Department of Electrical Engineering, Kyoto University
Katsura, Nishikyo, Kyoto 615-8510, Japan
‡School of Engineering, The University of Shiga Prefecture
2500 Hassaka-cho, Hikone, Shiga 522-8533, Japan
¶Osaka City University Advanced Mathematical Institute
3-3-138 Sughimoto, Sumiyoshi-ku, Osaka 558-8585, Japan
Email: kimura.masayuki.8c@kyoto-u.ac.jp

Abstract—Energy localized vibration in nonlinear lattices is known as intrinsic localized mode. The intrinsic localized mode can move without decaying its energy concentration. In this paper, behaviors of the moving intrinsic localized mode in a nonlinear lattice having two different regions are investigated. In particular, the transmission and the reflection at the junction of these two regions are focused on and discussed in detail.

1. Introduction

Intrinsic localized mode (ILM), which is a spatially localized and temporary periodic solution of nonlinear coupled oscillators, has been identified in various experimental systems [1]. Originally, the ILM is identified as a stationary oscillation of the nonlinear lattice [3, 2]. That is, the locus of ILM does not move. However, it is well known that ILM can move without decaying when an unstable ILM is perturbed to appropriate direction [4]. Such moving ILM is also observed experimentally in micro-cantilever arrays [5]. It implies that the moving ILM can be utilized as a carrier to transport kinetic energy in micro-/nano-engineering. So far, the interactions between the moving ILM and impurities are studied [6]. The transmission, reflection, and trapping phenomena are observed. This paper investigates the behavior of moving ILM at a junction of two different lattices. In particular, the velocity change after the moving ILM reach the junction is focused on. In Sec.2, the model equation and a static ILM are introduced. In Sec.3, the basic property of moving ILM is mentioned. The velocity changes are investigated and discussed in Sec.4. Finally, a brief summary of the result is shown in Sec.5.

2. Nonlinear lattice consisting of two regions

A nonlinear lattice, which is a mixed-model of the well-known Fermi-Pasta-Ulam (FPU) lattice and the nonlinear Klein-Gordon (NKG) lattice, is focused on in this paper. It is known that this type of the nonlinear lattice describes vibrations of coupled cantilever arrays [7, 5]. Motion of the tip of the nth cantilever u_n obeys the following equation:

$$\begin{aligned}\ddot{u}_n = &-\alpha_{1,n}u_n - \alpha_{2,n}(2u_n - u_{n+1} - u_{n-1}) \\ &- \beta_{1,n}u_n^3 - \beta_{2,n}(u_n - u_{n+1})^3 - \beta_{2,n}(u_n - u_{n-1})^3,\end{aligned} \tag{1}$$

where the linear on-site and coupling coefficients for the nth site are denoted by $\alpha_{1,n}$ and $\alpha_{2,n}$, respectively. The magnitude of cubic nonlinearity is represented by $\beta_{1,n}$ and $\beta_{2,n}$ for the on-site and the couping term, respectively. The total energy of the system is

$$\begin{aligned}\mathcal{H} = \sum_{n=1}^{N}\frac{1}{2}\dot{u}_n^2 + \sum_{n=1}^{N}\Big(&\frac{1}{2}\alpha_{1,n}u_n^2 + \frac{1}{4}\beta_{1,n}u_n^4 \\ &+ \frac{1}{2}\alpha_{2,n}(u_n - u_{n-1})^2 + \frac{1}{4}\beta_{2,n}(u_n - u_{n-1})^4\Big),\end{aligned} \tag{2}$$

where N is the total number of oscillators and is set at $N = 32$. In this paper, the periodic boundary conditions $u_{n+1} = u_1$ and $u_0 = u_n$ are assumed.

In Eq.(1), two types of ILM coexist. One has an amplitude distribution centered on a site. This site-center mode is called Sievers-Takeno mode (ST mode). The other is bond-center mode. Two neighboring oscillators have large amplitude and they oscillate anti-phase, which is called Page mode (P mode). Figure1(a) shows the amplitude distribution of an ST mode which is centered at $n = 6$. The parameters are set at $\alpha_{1,n} = 1$, $\alpha_{2,n} = 0.1$, $\beta_{1,n} = 1$, $\beta_{2,n} = 0.6$ for all n, and $\mathcal{H} = 2.5$. As shown in the figure, the energy is only distributed in a few sites.

The stability of ILMs depends on their spatial symmetry and the parameter ratio in the nonlinear coefficients $r_\beta = \beta_{2,n}/\beta_{1,n}$ [8]. If the ratio r_β is small, ST modes are stable whereas P modes are unstable. However, these stabilities are flipped when r_β becomes large. The threshold is around $r_\beta = 0.54$ for the case that $\alpha_{1,n} = 1$, $\alpha_{2,n} = 0.1$, $\beta_{1,n} = 1$ for all n, and $\mathcal{H} = 2.5$ [8]. As shown in Fig.1(b), one characteristic multiplier is located outside the unit circle. Thus, the ST mode is unstable.

3. Moving ILM

The position of the center of ILM does not change in time. However, it is known that unstable ILM begins to move with keeping its energy concentration if it is perturbed to appropriate direction [6]. The ILM traveling with almost constant velocity is called *moving ILM*. In this paper, to create moving ILMs, the eigenvectors $\boldsymbol{p}_\mathrm{s}$, $\boldsymbol{p}_\mathrm{u}$ corresponding to $\lambda_\mathrm{s} < 1$, $\lambda_\mathrm{u} > 1$, respectively, are used. The

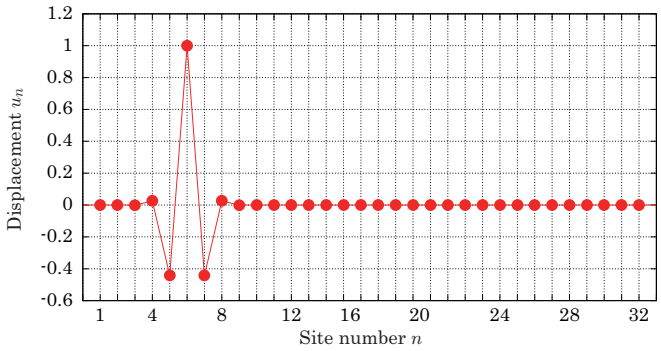

(a) ST mode

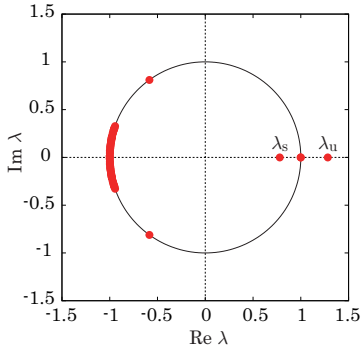

(b) Characteristic multipliers

Figure 1: ST mode standing at $n = 6$. The total energy is $\mathcal{H} = 2.5$. (a): Distribution of displacements when all the velocities are $\dot{u}_n = 0$. (b): Characteristic multiplies.

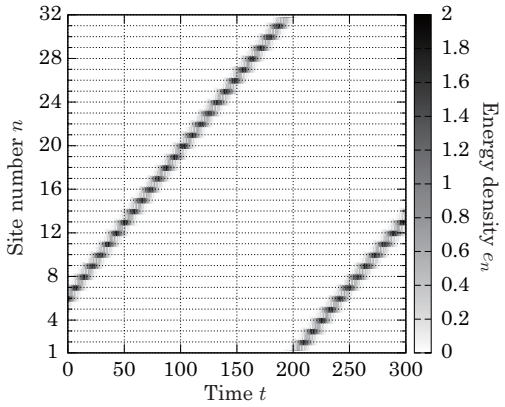

Figure 2: Energy distribution of the moving ILM. The perturbation parameter is set at $\epsilon = 2$. The velocity is about 0.14 sites per unit time.

initial condition of a moving ILM $\boldsymbol{u}_m$ is obtained as

$$\boldsymbol{u}_{\rm m} = \boldsymbol{u}_{\rm ST} + \epsilon(\boldsymbol{p}_{\rm u} + \boldsymbol{p}_{\rm s})/2, \tag{3}$$

where $\boldsymbol{u}_{\rm ST}$ represents the static ILM and $\epsilon > 0$ is the perturbation parameter. Figure2 shows the time course of the energy distribution of a moving ILM which is created with $\epsilon = 2$. The moving ILM has almost constant velocity and keeps its energy concentration during the simulation.

In order to extract the center of ILM, the following projection $\mathcal{G} : \mathbb{R}^{2N} \to \mathbb{C}$ is useful [9]:

$$h = \mathcal{G}(\boldsymbol{u}, \dot{\boldsymbol{u}}) = \sum_{n=1}^{N} \left\{ \left(\frac{1}{2}\dot{u}_n^2 + U_{{\rm On}}(u_n) \right) e^{i\frac{2\pi}{N}n} + U_{{\rm In}}(u_n - u_{n-1}) e^{i\frac{2\pi}{N}(n+\frac{1}{2})} \right\}, \tag{4}$$

where

$$U_{{\rm On}}(u_n) = \frac{1}{2}\alpha_{1,n}u_n^2 + \frac{1}{4}\beta_{1,n}u_n^4, \tag{5}$$

$$U_{{\rm In}}(u_n - u_{n-1}) = \frac{1}{2}\alpha_{2,n}(u_n - u_{n-1})^2 + \frac{1}{4}\beta_{2,n}(u_n - u_{n-1})^4. \tag{6}$$

The trajectories of the center of moving ILMs are shown in Fig.3. The slope becomes steep as the perturbation increases. The small fluctuation observed when the perturbation is small is due to the phase structure around static ILMs. A moving ILM started near an unstable ILM transits close to other unstable ILMs. The velocity is reduced when the moving ILM is close to the static unstable ILM [11]. To eliminate the effect of the small fluctuation of the velocity, the least square method is applied to estimate the slope of the trajectories. The resultant figure is shown in Fig.4. The velocity is almost proportional to the perturbation. The relationship between the velocity and the perturbation somewhat depends on the total energy. Static ILMs having higher energy become faster moving ILMs for the same perturbation. The plateaus appeared between $\epsilon = 1.5$ and 3 mean there is a parameter region where the moving ILM does not accelerated. It may be due to the phase structure, but it has not been clarified yet.

4. Transmission and reflection at the junction

In this section, the effect of parameter gap is investigated. One of parameters in Eq.(1) is changed for from the 17th to the 32nd site. The magnitude of the parameter gap is denoted by $\delta\bullet$, where $\bullet$ takes α_1, α_2, β_1, and β_2. Consider the nonlinear lattice having two different regions:

$$\alpha_{1,n} = 1,\ \alpha_{2,n} = 0.1,\ \beta_{1,n} = 1,\ \beta_{2,n} = 0.6, \qquad 1 \le n \le 16,$$
$$\alpha_{1,n} = 1,\ \alpha_{2,n} = 0.1,\ \beta_{1,n} = 1.02,\ \beta_{2,n} = 0.6, \quad 17 \le n \le 32.$$

In this case, the parameter gap is represented as $\delta\beta_1 = 0.02$. The trajectories when the case of $\delta\beta_1 = 0.02$ and -0.02 are shown in Figs.5(a) and 5(b). When the parameter gap is positive, all the moving ILMs are accelerated at the junction. On the other hand, the moving ILM is reflected at the junction when the parameter gap is negative and the velocity is small. In addition, the transmitting ILMs which originally have large velocities lose their velocity. The switch from the reflection to the transmission depends on the parameter gap. Figures.6(a)–6(d) shows the change of velocity ratio $r_{\rm v}$ in before and after the moving ILM reaches the junction. The case that $r_{\rm v}$ is unity means that

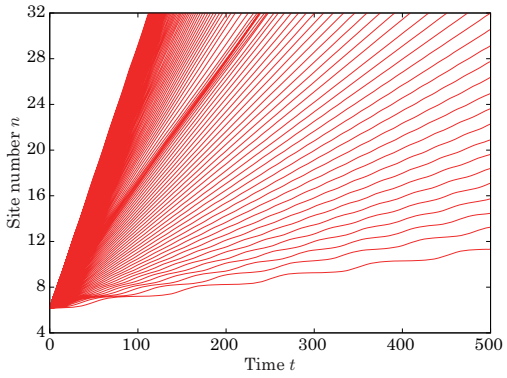

Figure 3: Trajectories of moving ILMs extracted by Eq.(4).

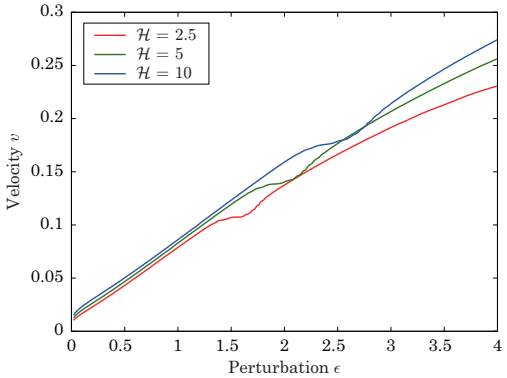

Figure 4: Relationship between the mean velocity and the perturbation. The mean velocity is obtained by using the least-square method which is applied to the trajectory data.

the moving ILM transmits the junction without gaining or losing the velocity. When the moving ILM is accelerated/deaccelerated, the ratio becomes $r_v > 1$ or $1 > r_v > 0$, respectively. For the perfect reflection, the ratio r_v takes -1.

As shown in the figures, the moving ILMs gain the velocity when the parameter gaps are positive. For the transmission, the ratio r_v converges to unity as the perturbation increases. It implies that the acceleration effect becomes relatively weak when the velocity of the moving ILM is large. The reflections appear only for the negative parameter gaps and the small perturbations. Since the velocity of the moving ILM is almost proportional to the perturbation, there exist a threshold velocity for each case to switch from the reflection to the transmission. The threshold velocity clearly increases with respect to the parameter gap. In addition, it depends on what parameter is changed. The threshold velocities for the case of Fig.6(a) and 6(d) are larger about twice as much as those of Fig.6(b) and 6(c) when the parameter is decreased about 10 % from the original value.

5. Conclusion

In this paper, the velocity change of moving ILMs at the junction of two different nonlinear lattices is discussed. As as result, the transmissions and the reflections are observed. For the cases that the parameter gaps are positive, the transmissions with acceleration are only observed. On the other hand, the transmissions with deacceleration and the reflection are observed for the negative parameter gaps. The moving ILM needs a threshold velocity to transmit the junction. The mechanism of appearing the threshold velocity is still unclear. We will investigate the mechanism in term of the change of phase structure with the linear or nonlinear coefficients. If the threshold velocity is able to be quite large, a transmission barrier against moving ILMs will be realized, *i.e.* rectifier of ILM. The rectifier of ILM would be applied to the thermal rectifiers, in which nonlinearity plays crucial role [10]. The authors hope to realize a thermal device using ILM in the future.

Acknowledgments

This work was supported by the Ministry of Education, Culture, Sports, Science and Technology in Japan, Grant-in-Aid for Young Scientist (B) No. 25820164.

References

[1] S. Flach and A. V. Gorbach, "Discrete breathers – advances in theory and applications," *Phys. Rep.*, vol.467, p.1–116, 2008.

[2] S. Takeno and A. J. Sievers, "Anharmonic resonant modes in perfect crystals," *Solid State Commun.*, vol.67, p.1023, 1988.

[3] J. B. Page, "Asymptotic solutions for localized vibrational modes in strongly anharmonic periodic systems," *Phys. Rev. B*, vol.41, p.7835, 1990.

[4] S. Flach and C. R. Willis, "Movability of localized excitations in nonlinear discrete systems: A separatrix problem," *Phys. Rev. Lett.*, vol.72, p.1777, 1994.

[5] M. Sato, B. E. Hubbard, A. J. Sievers, B. Ilic, D. A. Czaplewski, and H. G. Craighead, "Observation of locked intrinsic localized vibrational modes in a micromechanical oscillator array," *Phys. Rev. Lett.*, vol.90, p.044102, 2003.

[6] Y. Doi, "Sensitive behaviors of intrinsic localized modes in the presence of impurity and random inhomogeneity," *Wave Motion*, vol.38, p.177, 2003.

[7] T. Hikihara, K. Torii, and Y. Ueda, "Quasi-periodic wave and its bifurcation in coupled magneto-elastic beam system," *Phys. Lett. A*, vol.281, p.155, 2001.

[8] M. Kimura and T. Hikihara, "Stability change of intrinsic localized mode in finite nonlinear coupled oscillators," *Phys. Lett. A*, vol.372, p.4592, 2008.

[9] P. A. Houle, "Phase plane of moving discrete breathers," *Phys. Rev. E*, vol.56, p.3657, 1997.

[10] M. E. Manley, "Intrinsic Localized Lattice Modes and Thermal Transport: Potential Application in a Thermal Rectifier," *arXiv:0905.2988*, 2009.

[11] M. Kimura and T. Hikihara, "Capture and release of traveling intrinsic localized mode in coupled cantilever array," *Chaos*, vol.19, p.013138, 2009.

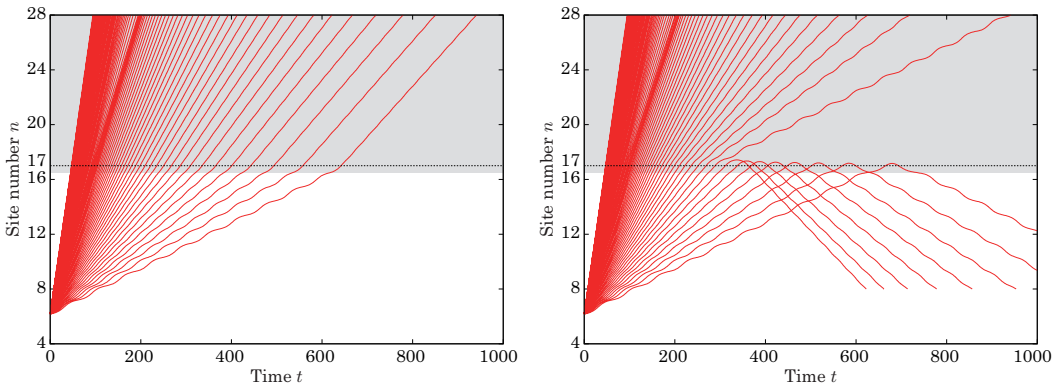

(a) transmission (b) transmission and reflection

Figure 5: Trajectories of moving ILMs. The coefficient of cubic nonlinearity $\beta_{1,n}$ changed for from the 17th to the 32nd oscillators. Dark regions indicate where the parameter is changed. (a) $\delta\beta_1 = 0.02$. (b) $\delta\beta_1 = -0.02$.

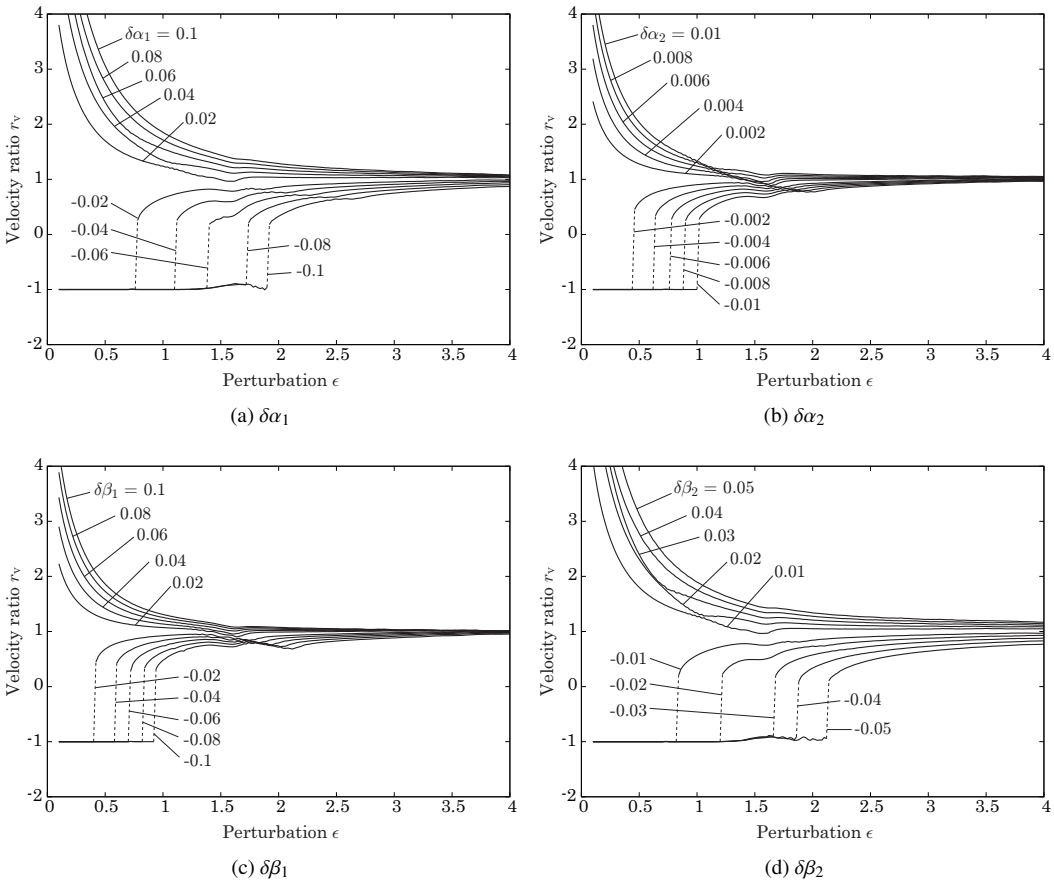

(a) $\delta\alpha_1$ (b) $\delta\alpha_2$

(c) $\delta\beta_1$ (d) $\delta\beta_2$

Figure 6: Velocity ratios for changing (a) linear on-site, (b) linear coupling, (c) nonlinear on-site, and (d) nonlinear coupling. The dashed lines are guide for eye.